

# Parameters of the lowest order chiral Lagrangian from fermion eigenvalues

Thomas DeGrand

*Department of Physics, University of Colorado, Boulder, CO 80309 USA*

Stefan Schaefer

*NIC, DESY, Platanenallee 6, D-15738 Zeuthen, Germany*

Recent advances in Random Matrix Theory enable one to determine the pseudoscalar decay constant from the response of eigenmodes of quenched fermions to an imaginary isospin chemical potential. We perform a pilot test of this idea, from simulations with two flavors of dynamical overlap fermions.

## I. INTRODUCTION

The leading-order chiral effective Lagrangian

$$\mathcal{L}_{\text{eff}} = \frac{F^2}{4} \text{Tr}(\partial_\mu U \partial^\mu U^\dagger) - \frac{\Sigma}{2} \text{Tr}[\mathcal{M}(U + U^\dagger)] \quad (1)$$

is characterized by two coupling constants,  $F$  and  $\Sigma$ . While they are fundamental from the point of the chiral Lagrangian, their values may be computed from the parent theory, QCD. This is a long-standing goal of lattice simulations.

$F$  and  $\Sigma$  are not measured directly in experiment: the values of the decay constant and condensate for nonzero quark mass are computed from the chiral Lagrangian through familiar functions of  $F$  and  $\Sigma$ , plus contributions from higher order terms in the chiral Lagrangian. Lattice simulations regularly present results for the mass-dependent quantities. Since it is not so easy to do simulations directly at zero quark mass (or at the physical up or down quark masses), the analysis of simulations typically involves fits of lattice data at several values of the quark mass to chiral perturbation theory formulas.  $F$  and  $\Sigma$  are parameters determined as part of the fit.

Many techniques for extracting the mass dependent parameters, or  $F$  and  $\Sigma$  themselves, have been devised. Most of them require studying the asymptotic behavior of correlation functions, and hence, need larger simulation volumes. However, in the epsilon regime ( $m_\pi L \ll 1$  but  $\Lambda L \gg 1$  for any other nonperturbative energy scale  $\Lambda$ ), properties of the chiral Lagrangian are encoded in the spectrum of low-lying eigenvalues of the QCD Dirac operator in a finite volume, whose distribution can be predicted by Random Matrix Theory (RMT) [1, 2, 3]. Many groups[4, 5, 6, 7, 8, 9, 10, 11, 12, 13, 14, 15, 16] have computed  $\Sigma$  from fits to the distributions of low-lying eigenmodes of the Dirac operator. This seems to require less computer power for equivalent accuracy[17] than “asymptotic” methods, and also seems to involve fits to data with fewer free parameters.

A method to compute  $F$  using eigenmodes was recently devised by G. Akemann, P. H. Damgaard, J. C. Osborn and K. Splittorff [18]. They imagine doing simulations in the epsilon-regime with two dynamical flavors, and then considering the spectrum of a partially quenched theory in which two non-dynamical flavors are coupled to an imaginary isospin chemical potential. The correlator of the ordinary eigenvalues with those of the quenched ones involves the product of the isospin chemical potential and  $F$ . The required eigenmode distributions are easily computed from an ordinary dynamical ensemble. This paper is a pilot study of the technique at lattice spacings which are small enough that one can imagine quoting a continuum number.

We can almost complete the calculation. The missing ingredient is actually analytic: We are doing the calculation in finite simulation volume. We know that finite volume alters the effective value of the condensate (said differently, the condensate appears in all relevant formulas multiplied by a volume-dependent coefficient) [19]. We expect that  $F$  is subject to similar modification. The precise calculation of this connection does not appear to have been performed, and appears to require more knowledge of chiral perturbation theory than we have. We return to this point below.

There have been two generations of previous variations of this idea, Refs. [20] and [21, 22]. These authors did simulations in which the isospin chemical potential was included in the action. This is of course much more expensive than what we are doing here.

We performed the calculation with lattice fermions which support the full  $SU(N_f) \otimes SU(N_f)$  chiral symmetry (including the anomalous singlet current and the index theorem), overlap fermions [23, 24]. We find doing overlap simulations to be reasonably straightforward. RMT makes predictions for QCD in fixed topological sectors and its predictions are for the pure imaginary eigenvalues of an anti-Hermitian Dirac operator. Both of these requirements are met unambiguously (modulo cutoff effects) by overlap fermions: the index theorem as realized by the Ginsparg-Wilson relation [25] gives the topology and the usual definition of the condensate as  $\Sigma = (1/Z)\partial Z/\partial m$  stereographically maps overlap eigenmodes onto the imaginary axis [26].

Typical high-statistics supercomputer collaborations (for example Ref. [27]) quote  $f_\pi$  with 0.3 per cent errors (but slightly greater errors for  $F$ ; see below). Ref. [21], which extracted  $F$  from eigenmodes (the isospin chemical potential is included in the simulation) has an 0.7 per cent error with about  $10^3$  samples. This was done deep in strong coupling so they did not attempt to make a continuum prediction. We will not come close to this amount of accuracy due to lack of statistics, but our results may not be uninteresting. Finding  $F$  does not seem necessarily to be a supercomputer project.

If we were doing simulations in the real world of three light flavors, what would we expect? Two representative continuum chiral perturbation theory fits to data give  $F = 88$  MeV [28] or  $F = 86.2 \pm 0.5$  MeV [29]. Our simulations are for two dynamical flavors and so strictly speaking we should not be talking about experimental comparisons. However, we will be unable to resist doing this.

The rest of the paper is organized as follows: We first review the observables we are going to compute and the corresponding Random Matrix predictions. Then we discuss the systematic and statistical uncertainties of this simulation, focusing on the corrections due to the finite volume. After that, the setup and results of our actual simulation will be given.

## II. THEORETICAL BACKGROUND

The key to the calculation is the connected correlation function between eigenvalues of the Dirac operator computed in the presence of a quenched chemical potential  $\lambda_j$ , and ordinary eigenvalues computed at zero chemical potential,  $\lambda_i$

$$\rho_{(1,1)}^{(2)conn}(x, y) = \left\langle \sum_i \delta(x - \lambda_i) \sum_j \delta(y - \lambda_j) \right\rangle - \left\langle \sum_i \delta(x - \lambda_i) \right\rangle \left\langle \sum_j \delta(y - \lambda_j) \right\rangle. \quad (2)$$

Eq. (3.49) of Ref. [18] gives the RMT prediction for this correlator in terms of the usual rescaled variables  $\hat{x} = \lambda_i \Sigma V$ ,  $\hat{y} = \lambda_j \Sigma V$ , the rescaled mass  $\hat{m} = m_q \Sigma V$ , and the rescaled isospin chemical potential  $\hat{\mu} = \hat{\delta} = \mu F \sqrt{V}$ .  $V$  is the volume.

$$\rho_{(1,1)}^{(2)conn}(\hat{x}, \hat{y}) = \hat{x}\hat{y} \frac{\begin{vmatrix} \mathcal{I}^+(\hat{y}, i\hat{m}) & J_\nu(i\hat{m}) & i\hat{m}J_{\nu+1}(i\hat{m}) \\ \mathcal{I}^+(\hat{y}, i\hat{m})' & J_\nu(i\hat{m})' & (i\hat{m}J_{\nu+1}(i\hat{m}))' \\ \mathcal{I}^+(\hat{y}, \hat{x}) & J_\nu(\hat{x}) & \hat{x}J_{\nu+1}(\hat{x}) \end{vmatrix} \begin{vmatrix} -\mathcal{I}^0(\hat{x}, i\hat{m}) & J_\nu(i\hat{m}) & i\hat{m}J_{\nu+1}(i\hat{m}) \\ -\mathcal{I}^0(\hat{x}, i\hat{m})' & J_\nu(i\hat{m})' & (i\hat{m}J_{\nu+1}(i\hat{m}))' \\ \tilde{\mathcal{I}}^-(\hat{x}, \hat{y}) & e^{-\hat{\delta}^2/2} J_\nu(\hat{y}) & e^{-\hat{\delta}^2/2} \hat{y} J_{\nu+1}(\hat{y}) \end{vmatrix}}{\begin{vmatrix} J_\nu(i\hat{m}) & i\hat{m}J_{\nu+1}(i\hat{m}) \\ J_{\nu-1}(i\hat{m}) & i\hat{m}J_\nu(i\hat{m}) \end{vmatrix}^2}, \quad (3)$$

The prime indicates the derivative with respect to  $i\hat{m}$ . This formula is the limit of a more general one with two non degenerate quark masses.  $\hat{x}$  and  $\hat{y}$  are the rescaled eigenmodes for  $\mu = 0$  and  $\mu = \delta$  respectively. The integrals are

$$\begin{aligned} \mathcal{I}^0(\hat{x}, \hat{y}) &\equiv \frac{1}{2} \int_0^1 dt J_\nu(\hat{x}\sqrt{t}) J_\nu(\hat{y}\sqrt{t}) = \frac{\hat{x}J_{\nu+1}(\hat{x}) J_\nu(\hat{y}) - \hat{y}J_{\nu+1}(\hat{y}) J_\nu(\hat{x})}{\hat{x}^2 - \hat{y}^2} \\ \mathcal{I}^\pm(\hat{x}, \hat{y}) &\equiv \frac{1}{2} \int_0^1 dt e^{\pm\hat{\delta}^2 t/2} J_\nu(\hat{x}\sqrt{t}) J_\nu(\hat{y}\sqrt{t}). \end{aligned} \quad (4)$$

Lattice data is never as beautiful as an analytic formula. In our case, the problems we face in applying Eq. 3 to simulation data are that

- We have limited statistics.

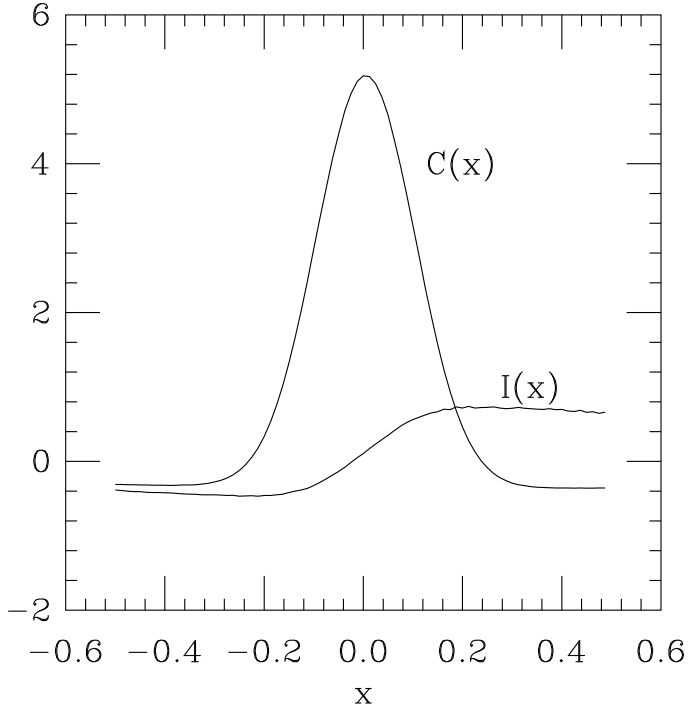


FIG. 1:  $C(x)$  and  $I(X)$  from Eqs. 5 and 6, for  $\mu = m\Sigma V = 2$ ,  $\zeta_{max}\Sigma V = 7$ ,  $\nu = 0$ .

- We do not compute a large number of eigenmodes.
- From our analysis of the integrated eigenvalue spectra we suspect that cutoff effects modify the spectrum of the higher modes away from the RMT prediction.
- Simulations are done in finite volume.

Each of the four points contributes to the systematic or statistical error of our final result.

The first problem on our list is the *limited statistics*. It makes the comparison of the measured eigenvalue data to the theoretical distribution of Eq. 3 difficult. It is therefore convenient to compute integrated correlators: The one suggested by Refs. [20] and [21] is

$$C(x, \zeta_{max}) = \int_0^{\zeta_{max}} dy \rho(x+y, y) . \quad (5)$$

To avoid binning the data, which is highly ambiguous given the low statistics, we perform a second integral and take instead

$$I(X, \zeta_{max}) = \int_{-\zeta_{max}}^X C(x, \zeta_{max}) dx . \quad (6)$$

The first integral  $C(x)$  shows a spike at  $x = 0$  whose width goes roughly as  $\delta^2$ . Then  $I(X)$  will show a sharp step at  $X = 0$ . This is illustrated in Fig. 1. (In practice, we have only studied  $I(X)$ .)

To deal with the second and third problems, we realize that for any finite  $\zeta_{max}$ , only a *finite number of eigenmodes* contribute to  $C(x)$  or  $I(X)$ . Since we will be measuring the eigenvalue correlations at tiny  $\delta$ , a plot of the individual eigenvalue distributions will easily reveal which modes saturate the correlator below a certain value  $\zeta_{max}$  of  $\lambda$ . An example is illustrated in Fig. 2. In this case  $m\Sigma V = 2$ . We see that for  $\zeta_{max}\Sigma V \leq 7$  only the two lowest modes contribute to the  $\nu = 0$  correlator, and similarly for  $\zeta_{max}\Sigma V = 8$  for  $|\nu| = 1$ .

Let us now come to the fourth problem. *Finite volume* typically modifies field theory correlation functions, because the propagators are altered by the boundary conditions. In the epsilon regime, finite volume also suppresses long-range order. To compute the correction to the condensate, one basically writes the Goldstone boson fields as  $U(x) =$

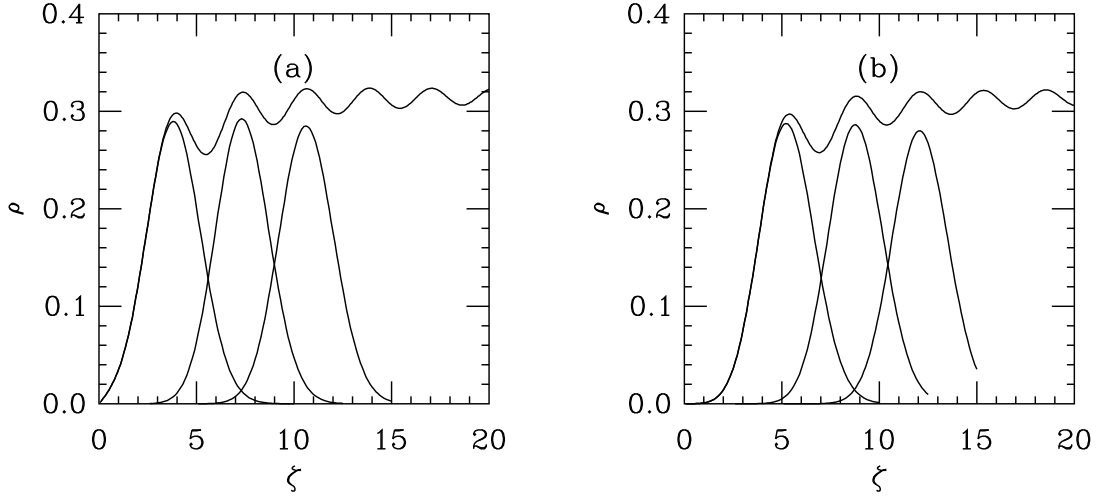


FIG. 2: An illustration of the RMT eigenvalue density (for all modes) and the distributions of single eigenvalues, for  $\mu = m\Sigma V = 2$  as a function of  $\hat{\zeta} = \lambda\Sigma V$ , in topological sectors (a)  $\nu = 0$ , (b)  $|\nu| = 1$ .

$U_0 \exp(i\pi(x)/F)$ , where  $U_0$  is the zero mode field which enters into all infinite-volume correlators (and is the variable connected to RMT formulas) and  $\pi(x)$  is small ( $\sim 1/L^{d+2}$  in  $d$ -dimensions). Then one expands the partition function to desired order in  $1/L$  and integrates out the small terms. For the condensate, the effect is to replace  $\Sigma$  by  $\Sigma_L = \rho_\Sigma \Sigma$  where

$$\rho_\Sigma = 1 + C_\Sigma \frac{1}{F^2} \Delta(0) + \dots \quad (7)$$

with  $\Delta(0)$  the contribution to the tadpole graph (propagator at zero separation) from finite-volume image terms. In the epsilon regime,  $\Delta(0) = -D/\sqrt{V}$  and  $D$  depends on the geometry[30]. (It is 0.1405 for hypercubes.) For  $N_f$  flavors,  $C_\Sigma = -(N_f^2 - 1)/N_f$ .

We are aware of no equivalent calculation appropriate to the case in hand. It amounts to computing corrections to derivatives of the partition function in the presence of a static background isospin vector potential. It includes both physical quarks (or pseudoscalar mesons) with ghost states.

However, at the end of the day, we want to make a comparison with phenomenology. We will make a guess (readers who do not like plausibility arguments are invited to look away for two paragraphs):

The epsilon-regime correction to  $\Sigma$  is the same as the one-loop correction in the p-regime, with the same  $C_\Sigma$ . All that differentiates the two is the evaluation of  $\Delta(0)$ . We will just assume that the same result obtains for  $F$  – that

$$F_L = \rho_F F \quad (8)$$

where  $\rho_F$  is the analog of  $\rho_L$  with  $C_F = -N_f/2$  replacing  $C_\Sigma$ .

Is this a plausible guess? Epsilon regime axial vector and vector current correlators in boxes of length  $T$  have been computed by several authors[31]. The mass-independent part of the correlator is a constant,

$$C(t) \sim \frac{F^2}{2T} \left[ 1 + \frac{N_f}{F^2} \left( \frac{D}{\sqrt{V}} - k \frac{T^2}{V} \right) \right]. \quad (9)$$

In a symmetric box ( $V = T^4$ ),  $k = D/2$  and the effect is equivalent to  $F_L = \rho_F F$  with  $C_F = -N_f/(2\sqrt{2})$ . Our guess scales properly with volume, but has a different factor. There is an additional  $1/\sqrt{V}$  correction in  $C(t)$ , which carries a nontrivial  $t$  dependence. It might be, that the effect of finite volume is to modify the functional dependence of Eq. 3. Clearly, we have exceeded the bounds of the numerical simulation we set out to do.

$ \nu $	N	mode 1	mode 2	mode 3
0	30	0.34	0.30	0.31
1	75	0.29	0.33	0.53

TABLE I: The quality factor of the individual modes for the result of a combined RMT fit to the lowest mode in each topological sector, see Fig. 3.

### III. NUMERICAL SIMULATION

Let us now come to the discussion of the actual simulation. Finding eigenmodes at nonzero isospin is easy: take a set of gauge configurations from the dynamical stream, rotate the time-like links

$$U_0(x) \rightarrow \exp(i\mu)U_0(x) \quad (10)$$

and re-compute eigenmodes of the massless Dirac operator. This (standard [32]) implementation insures that the chemical potential – and hence our extracted  $F$  – is not renormalized by lattice interactions.

Our version of the overlap uses various implementations of fat links, but as Eq. 10 is a global rotation, the fat links are rotated by the same amount. (That is, we first flatten the links, then rotate them.) And these quenched measurements of eigenvalues are basically “for free,” as compared to the cost of the generation of the configurations.

Our data set uses a lattice volume of  $12^4$  points. The lattice spacing  $a$ , as determined from the Sommer parameter  $r_0$  [33], is  $r_0/a = 3.71(5)$ . This calculation is “parasitic”; our main research program with our simulations involves heavier quark masses. We present data from the lightest quark mass at which we have extensive statistics,  $am_q = 0.03$ . The pseudoscalar mass is  $am_\pi = 0.329(3)$ . This is not in the epsilon regime, but experience shows RMT is robust enough to work well outside the epsilon regime, and anyway, we are just making a pilot study. In our conversions to physical units we use  $r_0 = 0.5$  fm.

The overlap operator uses a “kernel action” (the nonchiral action inserted in the usual overlap formula) with nearest and next-nearest (diagonal) neighbors. The  $12^4$  data set uses the differentiable hypercubic smeared link of Ref. [34]. Details of the actions are described in Refs. [13, 35, 36, 37]; everything except the choice of smearing for the link is identical to previous work.

Let us briefly summarize the algorithmic set-up of our computation. For the  $N_f = 2$  simulations we use the reflection/refraction algorithm first devised in Ref. [38]. In order to improve the tunneling rate and precondition the fermion determinant we use two additional heavy pseudo-fermion fields as suggested by Hasenbusch[39]. The integration is done with multiple-time scales[40]. The runs for all sea quark masses were performed within a few months on a cluster of 32 Opteron CPU’s which are connected by an Infiniband network. For the  $am_q = 0.03$  ensemble, we collected about 400 thermalized HMC trajectories of unit length and analyzed 30  $\nu = 0$  lattices and 75  $|\nu| = 1$  ones. We are computing eigenmodes using the “Primme” package of McCombs and Stathopoulos[41].

Our analysis begins with a determination of  $a^3\Sigma_L$  by fitting the RMT prediction of the distribution of the lowest eigenvalues of the Dirac operator without chemical potential to the data. As mentioned in the introduction, this method has been used by us and other groups during the last years and will serve as a cross check for the new method. Specifically, we fit the integrated eigenvalue density (cumulant)

$$P_i(\lambda) = \int_0^\lambda p_i(\lambda') d\lambda' \quad (11)$$

with  $p_i(\lambda)$  the density of the  $i$ -th lowest eigenmode. An example of a typical fit, this one to the lowest eigenmode in the  $\nu = 0$  and  $|\nu| = 1$  sectors, is shown in Fig. 3. Its best fit value is  $a^3\Sigma_L = 0.0073(3)$ , the quality factors for each individual mode from the combined fit are listed in Table I. Fits to other sets of eigenmodes produce entirely consistent results.

Now we proceed to the analysis of the eigenvalues with chemical potential and fits to Eq. 6. The correlator depends on two free parameters,  $\hat{\delta}$  and the scaled condensate (times volume)  $\Sigma V$ . The “experimental”  $I(X)$  varies almost continuously in  $X$  when there are many lattices in the data set. Since it is an integral, its values at different  $X$  are highly correlated. We account for correlations via a bootstrap analysis: We pick a bin size for  $X$  and make a set of bootstrap-averaged determinations of  $I(X_j, \zeta_{max})$ , with an uncertainty of a bin value  $\sigma_j$  determined from the

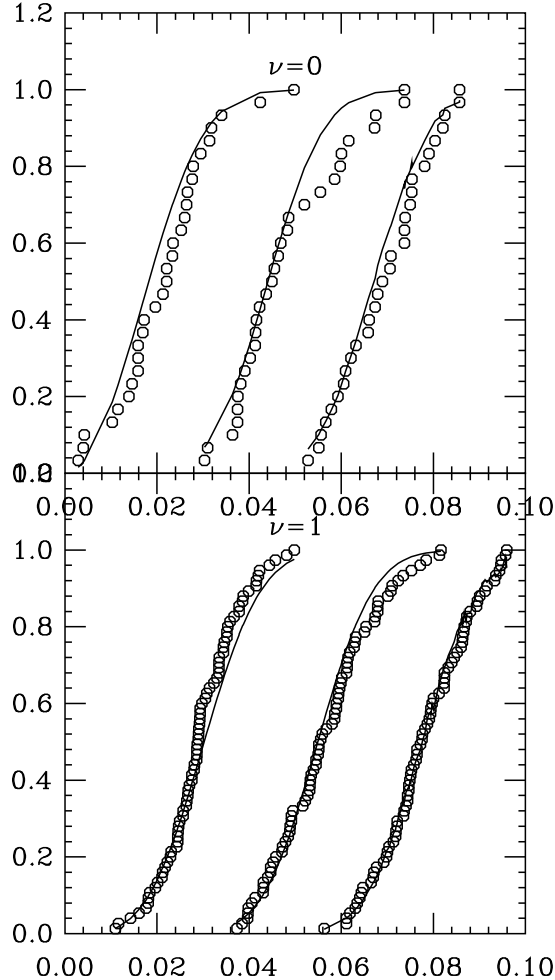


FIG. 3: Cumulant distribution for the three lowest eigenmodes (without chemical potential) in the  $|nu| = 0$  and  $1$  sectors, for our  $12^4 \beta = 7.3$   $am_q = 0.03$  data set. The curve is a fit to the lowest mode in  $\nu = 0$  and in  $|\nu| = 1$ , with  $a^3\Sigma_L = 0.0073$ .

bootstrap. Then we do a fit minimizing

$$\chi^2 = \frac{1}{N_b - 2} \sum_{j=1}^{N_b} \frac{(I(x_j) - I(x_j, \hat{\delta}, \Sigma V))^2}{\sigma_j^2}. \quad (12)$$

We determine uncertainties in the fit parameters from the fluctuations in a bootstrap average over a number of these fits. The fits involve a number of arbitrary choices, and our results should be independent of them. We have tested all of the following

- Range of  $\zeta_{max}$
- Range of  $X$ .
- Number of values of  $X_j$

The fit then determines a favored value of  $\hat{\delta}$ , from which  $F_L = \hat{\delta}/(\sqrt{V}\mu)$ . It also gives a second determination of the condensate  $\Sigma_L V$ , to be compared to the previously discussed direct fit to cumulant distributions.

The cumulant distribution of the eigenmodes tells us how many modes contribute for any  $\zeta_{max}$ . In this case, we believe that we can keep up to three eigenmodes and be consistent with random matrix theory predictions, so a maximum value will be someplace near the average value of the third eigenmode. This corresponds to a (not rescaled)  $\zeta_{max} = 0.07$  for  $\nu = 0$  and  $0.08$  for  $|\nu| = 1$ .

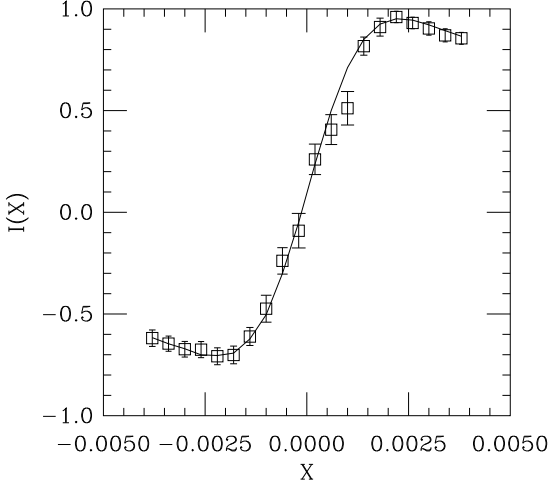


FIG. 4: Data (squares) and fit from  $|\nu| = 1$ . A cut  $\zeta_{max} = 0.07$  is enforced. The best fit values for this bootstrap sample are  $\Sigma_L V = 147$  and  $aF_L = 0.071$ .

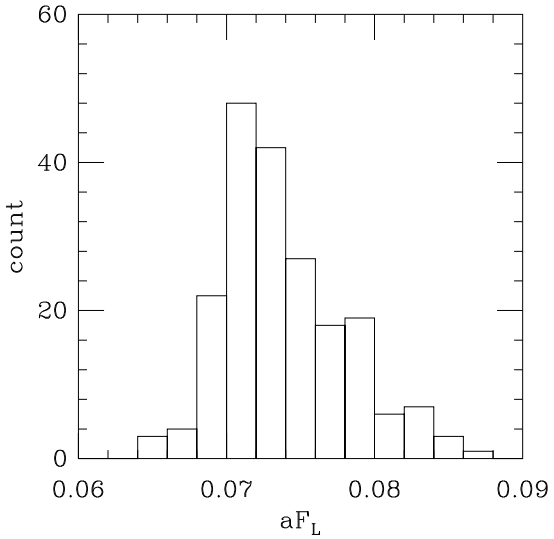


FIG. 5: Histogram of 200 bootstrap fits to  $aF_L$  from the  $|\nu| = 1$  data set:  $\zeta_{max} = 0.08$  and  $X = 0.004$  in the fits

Fig. 6 shows the dependence of fits on  $\zeta_{max}$ . These fits all include only the three lowest (but nonzero) eigenvalues in a topological sector. Smaller  $\zeta_{max}$  means that less data is included in the fit; larger  $\zeta_{max}$  means that more eigenmodes are needed to saturate the correlation function. It appears that results for this data set do not depend on the choice of  $\zeta_{max}$ .

Finally, a histogram of bootstrap values of the finite-volume decay constant  $F_L$  is shown in Fig. 5.

As the best-fit values do not show strong dependence on  $\zeta_{max}$  we choose to quote results from the  $\zeta_{max} = 0.08$  fit for the  $|\nu| = 1$  data set and  $\zeta_{max} = 0.07$  for  $\nu = 0$ . They give  $aF_L = 0.065(5)$  and  $a^3\Sigma_L = 0.0068(2)$ ; the  $|\nu| = 1$  set gives  $aF_L = 0.073(5)$  and  $a^3\Sigma_L = 0.0072(2)$ . Combining these fits gives  $aF_L = 0.069(4)$  and  $a^3\Sigma_L = 0.0071(1)$ . The fit gives a corroborating result for lattice-regulated  $\Sigma$ , consistent with our result from eigenmode cumulants.

To complete the calculation of  $\Sigma$ , we need to convert from lattice regularization to  $\overline{MS}$ . We do this using the intermediary of the RI-MOM scheme [43]. Our methodology is basically identical to what we did in Ref. [13].

We collected data from the three quark masses,  $am_q = 0.10, 0.05$ , and  $0.03$ . We took 40, 30, and 40 lattices, respectively. In RI-MOM, a Z-factor is basically the product of an averaged unamputated momentum-space vertex

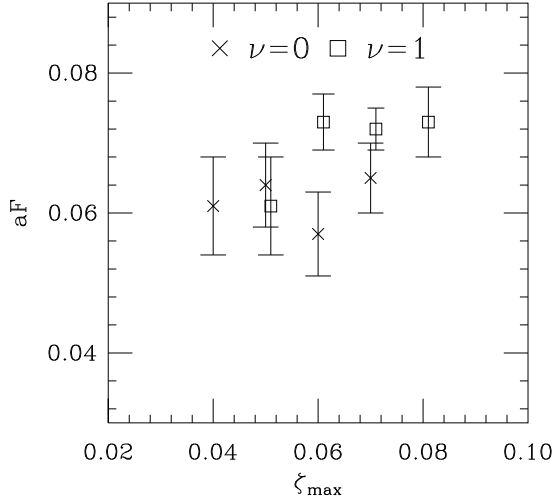


FIG. 6: Best-fit values of  $aF_L$ , varying  $\zeta_{max}$ .

function times two averaged inverse propagators, so for an N-lattice data set we formed N single-elimination jackknifed vertex-propagator combinations. The jackknife-averaged Z-factors are shown in Fig. 7(a).

We want the Z-factor at a fiducial scale  $\mu$  which conventionally is chosen to be 2 GeV. We fit the Z-factor for a particular mass to a linear dependence in  $\mu$  for  $\mu$ 's “nearby”  $\mu = 2$  GeV. There is one value for each possible value of lattice momentum. Combining all the points with the same value of  $\sum_i k_i^2$  gives a number with an error bar for a given value of  $\sum_i k_i^2$  for each of these jackknifed data sets.

We interpolate these fits to the desired value of  $\mu$ , 2 GeV with the lattice spacing taken from our Sommer parameter measurements. The uncertainty comes from jackknifing these results. For our simulations,  $\mu = 2$  GeV corresponds to  $a\mu \simeq 1.4$ , and we did fits over the range 1.0 or 1.1 to 1.6. (To be precise, 1.497 at  $am_q = 0.10$ , 1.45 at 0.05, 1.368 at 0.03.) The interpolated results are shown in Fig. 7(b). A linear fit gives the  $am_q = 0$  Z-factor of 0.656(28).

To convert to  $\overline{MS}$  scheme, we use the coupling constant from the so-called “ $\alpha_V$ ” scheme. The one-loop expression relating the plaquette to the coupling is

$$\ln \frac{1}{3} \text{Tr} U_p = -\frac{8\pi}{3} \alpha_V(q^*) W, \quad (13)$$

where  $W = 0.366$  and  $q^*a = 3.32$  for the tree-level Lüscher–Weisz action. All three data sets gave  $\alpha_V(q^*) = 0.188$ . The lattice spacing does not vary much in the three data sets, so converting any of them gives  $\alpha_s^{\overline{MS}}(2 \text{ GeV}) = 0.207$  and  $Z_S^{\overline{MS}}/Z_S^{RI'} = 1.158$ . Thus the combined lattice to  $\overline{MS}$  conversion factor is  $Z_S^{\overline{MS}}(2 \text{ GeV}) = 0.76(3)$ . We insert our lattice determination for  $aF_L$  in  $\rho_\Sigma$ . Dividing it out, we find

$$r_0 \Sigma(\overline{MS}, \mu = 2 \text{ GeV})^{1/3} = 0.594(13) \quad (14)$$

or

$$(\Sigma(\overline{MS}, \mu = 2 \text{ GeV}))^{1/3} = 234(4) \text{ MeV} \quad (15)$$

From the cumulant analysis,  $r_0 \Sigma(\overline{MS}, \mu = 2 \text{ GeV})^{1/3} = 0.600(13)$  or  $(\Sigma(\overline{MS}, \mu = 2 \text{ GeV}))^{1/3} = 237(6) \text{ MeV}$ . This seems to be quite consistent with other recent determinations [13, 14, 15, 17].

Now for  $F$ . Combining results for  $\nu = 0$  and  $|\nu| = 1$ , we find

$$r_0 F_L = 0.255(13) \quad (16)$$

or with  $r_0 = 0.5 \text{ fm}$ ,

$$F_L = 101(6) \text{ MeV}. \quad (17)$$

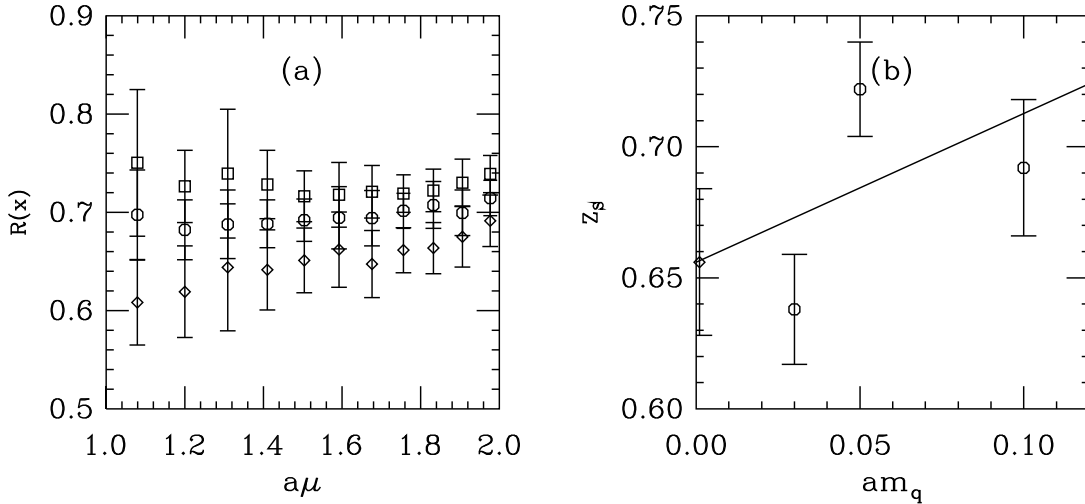


FIG. 7: (a)  $Z_S$  from our RI-MOM analysis: octagons are  $am_q = 0.10$ , squares, 0.05 and diamonds 0.03. Errors are from a jackknife average. (b)  $Z_S(RI')$  interpolated to  $\mu = 2$  GeV, vs  $am_q$ . The diamond shows the extrapolated point (with its error).

This is a little high compared to the phenomenological estimates of Refs. [28, 29]. There are ample reasons to suspect that some of this discrepancy could be due to fundamental problems with the simulation ( $N_f = 2$  is not real world), but we have already argued that we expect that  $F_L$  differs from  $F$ , by a factor which differs from unity by  $O(1/(F^2 L^2))$ .

Using the guess for finite value corrections,  $F_L = \rho_L F$ , and our guess for  $\rho_L$ , we estimate

$$r_0 F = 0.213(11) \quad (18)$$

or

$$F = 84(5)\text{MeV}. \quad (19)$$

Perhaps the error is more interesting than the central value: We have produced a six per cent statistical uncertainty for a full QCD quantity, with an extremely modest investment of computer power.

We remarked earlier that large scale simulations using asymptotic correlators typically produce calculations of  $f_\pi$  with small uncertainties but noisier predictions for  $F$ . As an example, MILC[44] quotes (their Table IV, Fit A, our conversion)  $r_1 F = 0.131(10)$  or  $F = 82(6)$  MeV. ( $r_1$  is defined through the heavy-quark force as  $r_1^2 F(r_1) = 1.0$ .) ETMC gets  $r_0 F = 0.197(2)$  [45]. We believe that our result used several orders of magnitude less computer power to produce a comparably-sized statistical error. Control over the systematic error due to the finite volume, however, remains a topic of future research.

#### IV. CONCLUSION

This was a pilot study, and it needs several ingredients before a complete calculation of  $F$  can be performed:

- A real analytic calculation of the finite volume correction to the eigenvalue correlator is needed. Is it of the form  $F_L = \rho_L F$  as we assumed, and if so, what is  $\rho_F$ ? In the absence of such a calculation, simulations at several volumes will be needed.
- A real numerical calculation needs to truly enter the epsilon regime, through a combination of lower pseudoscalar mass and larger volume.
- The best way we know to extract the condensate from Dirac eigenmodes used the distribution of individual eigenmodes, not the sum over many modes. The analog for  $F$  would be a calculation of the correlator of one eigenmode of ordinary fermions with one eigenmode of partially quenched fermions in an isospin chemical potential. We understand [46] that such a calculation is in progress.

- Finally, while we said at the beginning of this paper that  $F$  apparently does not need to be a supercomputing project, finding the physical decay constants involves determining higher-order coefficients in the chiral Lagrangian. At present, this can only be done in a spectroscopy-type calculation, from the asymptotic behavior of a correlation function. This can be expensive. Is there a way [47] to remove that bottleneck by relating these coefficients to some property of Dirac eigenmodes?

### Acknowledgments

This work was supported in part by the US Department of Energy. T. D. would like to thank Poul Damgaard for encouraging him to attempt this calculation and for much valuable advice. He would also like to thank Kim Splittorff for clarifying correspondence. We would like to thank Hidenori Fukaya and Silvia Necco for their comments on finite volume corrections.

---

- [1] E. V. Shuryak and J. J. M. Verbaarschot, Nucl. Phys. A **560**, 306 (1993) [arXiv:hep-th/9212088].
- [2] J. J. M. Verbaarschot and I. Zahed, Phys. Rev. Lett. **70**, 3852 (1993) [arXiv:hep-th/9303012].
- [3] J. J. M. Verbaarschot, Phys. Rev. Lett. **72**, 2531 (1994) [arXiv:hep-th/9401059].
- [4] M. E. Berbenni-Bitsch, S. Meyer, A. Schäfer, J. J. M. Verbaarschot and T. Wettig, Phys. Rev. Lett. **80**, 1146 (1998) [arXiv:hep-lat/9704018].
- [5] P. H. Damgaard, U. M. Heller and A. Krasnitz, Phys. Lett. B **445**, 366 (1999) [arXiv:hep-lat/9810060].
- [6] M. Göckeler, H. Hehl, P. E. L. Rakow, A. Schäfer and T. Wettig, Phys. Rev. D **59**, 094503 (1999) [arXiv:hep-lat/9811018].
- [7] R. G. Edwards, U. M. Heller, J. E. Kiskis and R. Narayanan, Phys. Rev. Lett. **82**, 4188 (1999) [arXiv:hep-th/9902117].
- [8] L. Giusti, M. Lüscher, P. Weisz and H. Wittig, JHEP **0311**, 023 (2003) [arXiv:hep-lat/0309189].
- [9] E. Follana, A. Hart, C. T. H. Davies and Q. Mason [HPQCD Collaboration], Phys. Rev. D **72**, 054501 (2005) [arXiv:hep-lat/0507011].
- [10] M. E. Berbenni-Bitsch, S. Meyer and T. Wettig, Phys. Rev. D **58**, 071502 (1998) [arXiv:hep-lat/9804030].
- [11] P. H. Damgaard, U. M. Heller, R. Niclasen and K. Rummukainen, Phys. Lett. B **495**, 263 (2000) [arXiv:hep-lat/0007041].
- [12] T. DeGrand, R. Hoffmann, S. Schaefer and Z. Liu, Phys. Rev. D **74**, 054501 (2006) [arXiv:hep-th/0605147].
- [13] T. DeGrand, Z. Liu and S. Schaefer, Phys. Rev. D **74**, 094504 (2006) [Erratum-ibid. D **74**, 099904 (2006)] [arXiv:hep-lat/0608019].
- [14] C. B. Lang, P. Majumdar and W. Ortner, Phys. Lett. B **649**, 225 (2007) [arXiv:hep-lat/0611010].
- [15] H. Fukaya *et al.* [JLQCD Collaboration], Phys. Rev. Lett. **98**, 172001 (2007) [arXiv:hep-lat/0702003].
- [16] H. Fukaya *et al.*, arXiv:0705.3322 [hep-lat].
- [17] Compare the summaries in C. McNeile, Phys. Lett. B **619**, 124 (2005) [arXiv:hep-lat/0504006].
- [18] G. Akemann, P. H. Damgaard, J. C. Osborn and K. Splittorff, Nucl. Phys. B **766**, 34 (2007) [arXiv:hep-th/0609059].
- [19] J. Gasser and H. Leutwyler, Phys. Lett. B **188**, 477 (1987).
- [20] P. H. Damgaard, U. M. Heller, K. Splittorff and B. Svetitsky, Phys. Rev. D **72**, 091501 (2005) [arXiv:hep-lat/0508029].
- [21] P. H. Damgaard, U. M. Heller, K. Splittorff, B. Svetitsky and D. Toublan, Phys. Rev. D **73**, 074023 (2006) [arXiv:hep-lat/0602030].
- [22] P. H. Damgaard, U. M. Heller, K. Splittorff, B. Svetitsky and D. Toublan, Phys. Rev. D **73**, 105016 (2006) [arXiv:hep-th/0604054].
- [23] H. Neuberger, Phys. Lett. B **417**, 141 (1998) [arXiv:hep-lat/9707022].
- [24] H. Neuberger, Phys. Rev. Lett. **81**, 4060 (1998) [arXiv:hep-lat/9806025].
- [25] P. H. Ginsparg and K. G. Wilson, Phys. Rev. D **25**, 2649 (1982).
- [26] F. Niedermayer, Nucl. Phys. Proc. Suppl. **73**, 105 (1999) [arXiv:hep-lat/9810026].
- [27] C. Bernard *et al.* [MILC Collaboration], arXiv:hep-lat/0609053.
- [28] J. Gasser and H. Leutwyler, Annals Phys. **158**, 142 (1984).
- [29] G. Colangelo and S. Durr, Eur. Phys. J. C **33**, 543 (2004) [arXiv:hep-lat/0311023].
- [30] J. Gasser and H. Leutwyler, Phys. Lett. B **184**, 83 (1987); Nucl. Phys. B **307**, 763 (1988). See also P. Hasenfratz and H. Leutwyler, Nucl. Phys. B **343**, 241 (1990).
- [31] A partial citation path includes F. C. Hansen, Nucl. Phys. B **345**, 685 (1990); F. C. Hansen and H. Leutwyler, Nucl. Phys. B **350**, 201 (1991); P. H. Damgaard, P. Hernandez, K. Jansen, M. Laine and L. Lellouch, Nucl. Phys. B **656**, 226 (2003) [arXiv:hep-lat/0211020]; P. Hernandez and M. Laine, JHEP **0301**, 063 (2003) [arXiv:hep-lat/0212014].

- [32] P. Hasenfratz and F. Karsch, Phys. Lett. B **125**, 308 (1983).
- [33] R. Sommer, Nucl. Phys. B **411**, 839 (1994) [arXiv:hep-lat/9310022].
- [34] A. Hasenfratz, R. Hoffmann and S. Schaefer, JHEP **0705**, 029 (2007) [arXiv:hep-lat/0702028].
- [35] T. A. DeGrand [MILC collaboration], Phys. Rev. D **63**, 034503 (2001) [arXiv:hep-lat/0007046].
- [36] T. A. DeGrand and S. Schaefer, Phys. Rev. D **71**, 034507 (2005) [arXiv:hep-lat/0412005].
- [37] T. DeGrand and S. Schaefer, JHEP **0607**, 020 (2006) [arXiv:hep-lat/0604015].
- [38] Z. Fodor, S. D. Katz and K. K. Szabo, JHEP **0408**, 003 (2004) [arXiv:hep-lat/0311010].
- [39] M. Hasenbusch, Phys. Lett. B **519**, 177 (2001) [arXiv:hep-lat/0107019].
- [40] C. Urbach, K. Jansen, A. Shindler and U. Wenger, Comput. Phys. Commun. **174**, 87 (2006) [arXiv:hep-lat/0506011].
- [41] A. Stathopoulos, Nearly optimal preconditioned methods for hermitian eigenproblems under limited memory. Part I: Seeking one eigenvalue, Tech Report: WM-CS-2005-03, July, 2005. To appear in SIAM J. Sci. Comput. A. Stathopoulos and J. R. McCombs, Nearly optimal preconditioned methods for hermitian eigenproblems under limited memory. Part II: Seeking many eigenvalues, Tech Report: WM-CS-2006-02, June, 2006.
- [42] C. W. Bernard *et al.*, Phys. Rev. D **62**, 034503 (2000) [arXiv:hep-lat/0002028].
- [43] G. Martinelli, C. Pittori, C. T. Sachrajda, M. Testa and A. Vladikas, Nucl. Phys. B **445**, 81 (1995) [arXiv:hep-lat/9411010].
- [44] C. Aubin *et al.* [MILC Collaboration], Phys. Rev. D **70**, 114501 (2004) [arXiv:hep-lat/0407028].
- [45] Ph. Boucaud *et al.* [ETM Collaboration], Phys. Lett. B **650**, 304 (2007) [arXiv:hep-lat/0701012].
- [46] G. Akemann and P. H. Damgaard, private communication about work in progress.
- [47] For an example of a related discussion, see G. Akemann and P. H. Damgaard, Phys. Lett. B **583**, 199 (2004) [arXiv:hep-th/0311171].